Electronic and Structural Investigations of Technetium Compounds by X-ray Absorption Spectroscopy

Ilham Almahamid,[†] Jeffrey C. Bryan,[‡] Jerome J. Bucher,[§] Anthony K. Burrell,[‡] Norman M. Edelstein,*[,§] Eric A. Hudson,[||] Nikolas Kaltsoyannis,[§] Wayne W. Lukens,[§] David K. Shuh,*[,§] Heino Nitsche,[⊥] and Tobias Reich[⊥]

Earth Sciences Division, Lawrence Berkeley Laboratory, Berkeley, California 94720, Inorganic and Structural Chemistry Group, Los Alamos National Laboratory, Los Alamos, New Mexico 87545, Chemical Sciences Division, Lawrence Berkeley Laboratory, Berkeley, California 94720, G. T. Seaborg Institute for Transactinium Science, Lawrence Livermore National Laboratory, Livermore, California 94551, and Institut für Radiochemie, Forschungszentrum Rossendorf e. V., Postfach 51 01 19, D-01314 Dresden, Germany

Received July 19, 1994[⊗]

X-ray absorption near edge structure spectroscopy has been used to establish the chemical shifts of the technetium K edge in a range of compounds containing Tc in a variety of formal oxidation states. The edge positions span 19.9 eV from Tc metal to NH_4TcO_4. Strong correlation between chemical shift and formal oxidation state is observed. Extended X-ray absorption fine structure (EXAFS) spectroscopy of $Tc_2(CO)_{10}$ indicates that multiple scattering along the Tc−C−O vector is more important than direct Tc···O scattering. TcO_2 is shown by EXAFS to possess a distorted rutile structure with a closest Tc−Tc distance of 2.61 Å. This is rationalized in terms of the Goodenough model for bonding in transition metal dioxides.

Introduction

X-ray absorption spectroscopy (XAS) is a well established technique for the determination of oxidation state and local chemical environment.[1] It is particularly well suited to the study of radioactive and hazardous materials in that its high sensitivity facilitates study of dilute samples, both solutions and amorphous materials. Furthermore, in the hard X-ray regime the samples may be safely contained for *in situ* measurements at storage ring facilities. Thus XAS provides an ideal means for electronic and structural investigations of fission products and other environmentally relevant systems.

^{99}Tc is a byproduct of nuclear fission, and its significant half-life ($t_{1/2} = 2.13 \times 10^5$ years) necessitates its consideration in the long-term disposal of nuclear waste.[2] The principal Tc-containing component of nuclear wastes is TcO_4^-, and the propensity of TcO_4^- to migrate in the geosphere[3] has led to research aimed at the facile conversion of pertechnetate into other, less mobile compounds of ^{99}Tc.[4] We recently reported an X-ray absorption near edge structure (XANES) spectroscopic evaluation of the efficacy of a process designed to reduce TcO_4^- to TcO_2 in wasteform cement.[5] The form of the XANES spectra and the chemical shifts of the Tc K edge in TcO_4^-, TcO_2, and Tc metal were employed to establish the oxidation state of Tc. This paper describes the extension of our XANES investigation to a wider range of Tc compounds, with examples drawn from formal oxidation states 0, +2, +4, +5, and +7. The structural characterization of $Tc_2(CO)_{10}$ and TcO_2 by extended X-ray absorption fine structure (EXAFS) spectroscopy is also reported. In the case of the latter, our results provide the first detailed structural information.

Experimental Section

The XAS measurements were performed at the storage ring of the Stanford Synchrotron Radiation Laboratory (SSRL) on wiggler beamlines 4-3 and 4-1. Tc K edge (~21.05 keV) spectra were recorded with Si(220) monochromator crystals (detuned 50% to reduce higher order harmonic content). The convoluted experimental resolution is estimated at ~3 eV. Ionization chamber detectors were used for transmission experiments, and fluorescence measurements were performed with a Stearn Heald detector along with either a single element Si detector or a 4 pixel, single-element Ge detector. All spectra were collected simultaneously with NH_4TcO_4 as a reference to establish the respective chemical shifts and to ensure photon energy calibrations. Edge positions were determined using the first-derivative method.[6] Data analysis was performed with the EXAFSPAK program suite, written by Graham N. George of the SSRL.

NH_4TcO_4 was purchased from Oak Ridge National Laboratory. TcO_2 was prepared by thermal decomposition of NH_4TcO_4.[7] $Tc_2(CO)_{10}$,[8] $Tc(ArN)_3I$ (ArN = 2,6-$Pr^i_2C_6H_3N$),[9] $[Tc(ArN)_3]_2Hg$,[10] $[TcCl_2(PMe_2Ph)_2]_2$,[11] and $TcCl_2(py)_4$ (py = C_5H_5N)[12] were prepared according to the literature procedures.

Solutions of $Tc_2(CO)_{10}$ (0.2 M in toluene), $[TcCl_2(PMe_2Ph)_2]_2$ (0.08 M in THF), $TcCl_2(py)_4$ (0.1 M in toluene), $Tc(ArN)_3I$ (0.1 M in toluene),

[†] Earth Sciences Division, Lawrence Berkeley Laboratory.
[‡] Los Alamos National Laboratory.
[§] Chemical Sciences Division, Lawrence Berkeley Laboratory.
[||] Lawrence Livermore National Laboratory.
[⊥] Forschungszentrum Rossendorf.
[⊗] Abstract published in *Advance ACS Abstracts,* December 1, 1994.

(1) *X-ray Absorption. Principles, Applications and Techniques of EXAFS, SEXAFS and XANES*; Koningsberger, D. C., Prins, R., Eds.; John Wiley and Sons, Inc.: New York, 1988.
(2) Lieser, K. H. *Radiochim. Acta* **1993**, *63*, 5.
(3) Meyer, R. E.; Arnold, W. D.; Case, F. I.; O'Kelley, G. D. *Radiochim. Acta* **1991**, *55*, 11.
(4) Langton, C. A. In Proceedings of the Ninth Annual DOE Low-level Waste Management Conference, Denver, CO, 1987.
(5) Shuh, D.; Kaltsoyannis, N.; Bucher, J. J.; Edelstein, N. M.; Clark, S. B.; Nitsche, H.; Reich, T.; Almahamid, I.; Torretto, P.; Lukens, W.; Roberts, K.; Hudson, E. A.; Yee, B. C.; Carlson, D. E.; Yee, A.; Buchanan, B. B.; Leighton, T.; Yang, W.-S.; Bryan, J. C. *Mater. Res. Soc. Symp. Proc.*, in press.
(6) Sayers, D. E., Bunker, B. A. in ref 1, p 211.
(7) Lieser, K. H.; Bauscher, Ch.; Nakashima, T. *Radiochim. Acta* **1987**, *42*, 191.
(8) Herrmann, W. A.; Alberto, R.; Bryan, J. C.; Sattelberger, A. P. *Chem. Ber.* **1991**, *124*, 1107.
(9) Bryan, J. C.; Burrell, A. K.; Miller, M. M.; Smith, W. H.; Burns, C. J.; Sattelberger, A. P. *Polyhedron* **1993**, *12*, 1769.
(10) Burrell, A. K.; Clark, D. L.; Gordon, P. L.; Sattelberger, A. P.; Bryan, J. C. *J. Am. Chem. Soc.* **1994**, *116*, 3813.
(11) Burns, C. J.; Burrell, A. K.; Cotton, F. A.; Haefner, S. C.; Sattelberger, A. P. *Inorg. Chem.* **1994**, *33*, 2257.
(12) Barrera, J.; Burrell, A. K.; Bryan, J. C. Manuscript in preparation.

0020-1669/95/1334-0193$09.00/0

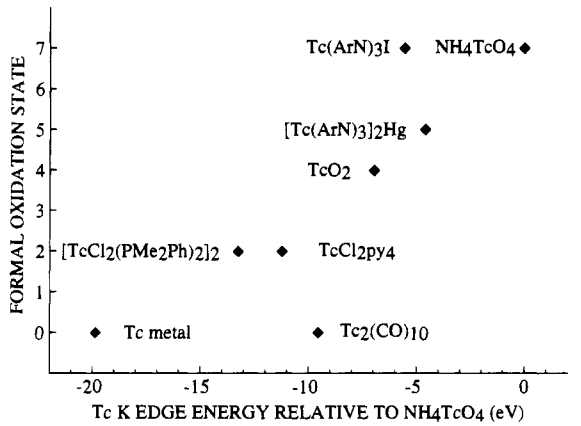

Figure 1. Chemical shifts of the Tc K edge versus formal oxidation state for Tc metal, $[TcCl_2(PMe_2Ph)_2]_2$, $TcCl_2(py)_4$ (py = C_5H_5N), $Tc_2(CO)_{10}$, TcO_2, Tc(ArN)$_3$I (ArN = 2,6-$Pr^i_2C_6H_3N$), $[Tc(ArN)_3]_2Hg$, and NH_4TcO_4. All XANES spectra were acquired with NH_4TcO_4 as a reference, and the chemical shifts are therefore reported relative to NH_4TcO_4.

Table 1. Shifts in the Technetium K Absorption Edge Relative to NH_4TcO_4

Tc compd	K edge shift (eV)	formal oxidn state	Tc compd	K edge shift (eV)	formal oxidn state
NH_4TcO_4	0	7	$Tc_2(CO)_{10}$	−9.55	0
$[Tc(ArN)_3]_2Hg$	−4.61	5	$TcCl_2(py)_4$	−11.21	2
Tc(ArN)$_3$I	−5.57	7	$[TcCl_2(PMe_2Ph)_2]_2$	−13.24	2
TcO_2	−6.95	4	Tc metal	−19.85	0

$[Tc(ArN)_3]_2Hg$ (0.05 M in toluene), and NH_4TcO_4 (~0.1 M in water) were placed in 10 mm outside diameter thin-walled silica NMR tubes to a depth of *ca.* 1 cm. The tubes were subsequently encased in protective polyethylene shrink wrap. TcO_2 was prepared for XAS as a solid mixture with graphite and packaged in the same manner as the liquid samples.

Results and Discussion

(a) Chemical Shifts of the Tc K Edge. K edge XANES spectra were obtained for eight Tc systems: Tc metal, $Tc_2(CO)_{10}$, $[TcCl_2(PMe_2Ph)_2]_2$, $TcCl_2(py)_4$ (py = C_5H_5N), TcO_2, Tc(ArN)$_3$I (ArN = 2,6-$Pr^i_2C_6H_3N$), $[Tc(ArN)_3]_2Hg$, and NH_4TcO_4. The shifts in the edge positions relative to NH_4TcO_4 are shown in Figure 1 and collected in Table 1, and it is clear that there is a strong correlation between formal oxidation state and K edge position. An increase in formal oxidation state implies an increase in effective charge, and it has been shown that X-ray absorption edge energies are governed mainly by the effective charge on the absorbing atom or ion.[13] In general, chemical shifts are toward the high-energy side of the elemental edge and increase progressively with the formal oxidation state of the absorbing atom,[14] as our Tc data illustrate.

Unlike core level X-ray photoelectron spectroscopy (XPS), XANES is not a direct method for the determination of binding energies. XANES spectra do not have characteristic signatures at the ionization energy as the oscillator strength is contained predominantly in transitions to discrete bound states and multiple scattering resonances in the continuum.[15] Thus the quantitative use of XAS edge shifts to determine chemical valence and effective charge is less precise than equivalent comparisons of XPS binding energies. These have been determined for the Tc $3d_{5/2}$ atomic orbital (AO) in a wide range of Tc compounds,[16] together with the shifts in the $K\alpha_1$ ($2p_{3/2} \rightarrow 1s$) emission line.[17] Both data sets show strong correlation with the effective charge on the metal atom.

Nevertheless, the 19.9 eV K edge shift between Tc metal and NH_4TcO_4 (not an unusual value for transition metals[13]) provides a substantial range over which the relationship of oxidation state to absorption edge energy may be examined. Of the eight systems studied, six display an almost linear relationship, with $Tc_2(CO)_{10}$ and Tc(ArN)$_3$I showing more significant differences. $[TcCl_2(PMe_2Ph)_2]_2$ and $TcCl_2(py)_4$ contain Tc as Tc(II), and their edge positions are 13.2 and 11.2 eV, respectively, lower than that of NH_4TcO_4. That $[TcCl_2(PMe_2Ph)_2]_2$ has a 2.0 eV greater shift than $TcCl_2(py)_4$ may be a result of the stronger σ-donor and weaker π-acceptor nature of PMe_2Ph versus C_5H_5N.

Both Tc(ArN)$_3$I and NH_4TcO_4 contain Tc in a formal oxidation state of +7, but Tc(ArN)$_3$I has a Tc K edge energy which is 5.6 eV lower than that of NH_4TcO_4. This is probably a reflection of the relative electron-withdrawing properties of the ligands in each case, with the oxygens inducing a greater effective charge on the Tc than the ArN/I combination. The magnitude of the difference is somewhat surprising, as Tc(ArN)$_3$I has an edge position which is further from NH_4TcO_4 than the Tc(V) $[Tc(ArN)_3]_2Hg$. In light of the preceding discussion, however, it is impossible to determine if this discrepancy is a genuine indication of differences in the effective charge at the metal atom.

The most significant deviation from the formal oxidation state/K edge energy relationship is that of $Tc_2(CO)_{10}$, which has an edge position closer to NH_4TcO_4 than either $TcCl_2(py)_4$ or $[TcCl_2(PMe_2Ph)_2]_2$. This is almost certainly the result of the electron-withdrawing ability of the carbonyl unit, and indicates that π back-bonding from metal to ligand dominates ligand to metal σ donation. Our results are entirely consistent with previous XPS measurements on $Cr(CO)_6$[18] and $Mn_2(CO)_{10}$,[19] which show the binding energy of the metal $2p_{3/2}$ AO to be close to that in MO_2 and well removed from the value obtained in the pure element.

(b) EXAFS Studies. (i) $Tc_2(CO)_{10}$. Although the structure of $Tc_2(CO)_{10}$ is known from X-ray crystallography,[20] it was decided to investigate its EXAFS with a view to assessing the contribution of multiple scattering pathways to the absorption modulations. The importance of multiple scattering paths in the EXAFS of systems containing backscatterers in a collinear configuration is well documented,[21−24] and we have observed

(13) Ghatikar, M. N.; Padalia, B. D. *J. Phys. C* **1978**, *11*, 1941.
(14) Agarwal, B. K. *X-Ray Spectroscopy*, 2nd ed.; Springer-Verlag: Berlin, 1991.
(15) Bianconi, A. In *X-ray Absorption. Principles, Applications and Techniques of EXAFS, SEXAFS and XANES*; Koningsberger, D. C., Prins, R., Eds.; John Wiley and Sons, Inc: New York, 1988; pp 573−662.
(16) Makarov, L. L.; Kryutchkov, S. V.; Zaitsev, Y. M.; Sablina, N. O.; German, K. E.; Kuzina, A. F. In *Technetium and Rhenium in Chemistry and Nuclear Medicine 3*; Nicolini, M., Ed.; Cortina International: Verona, 1990; pp 265−273.
(17) Makarov, L. L.; Kryutchkov, S. V.; Sablina, N. O.; Zaitsev, Y. M.; German, K. E.; Kuzina, A. F.; Spitsyn, V. I. *Dokl. Akad. Nauk SSSR* **1989**, *307*, 655.
(18) Pignataro, S.; Foffani, A.; Distefano, G. *Chem. Phys. Lett.* **1973**, *20*, 351.
(19) Van der Vondel, D. F.; Wuyts, L. F.; Van der Kelen, G. P.; Bevernage, L. *J. Electron. Spectrosc. Relat. Phenom.* **1977**, *10*, 389.
(20) Bailey, M. F.; Dahl, L. F. *Inorg. Chem.* **1965**, *4*, 1140.
(21) Teo, B. K. *J. Am. Chem. Soc.* **1981**, *103*, 3990.
(22) Garcia, J.; Delrio, M. S.; Buratini, E.; Benfatto, M. *Physica B* **1989**, *158*, 409.
(23) Vedrinskii, R. V.; Bugaev, L. A.; Levin, I. G. *Physica B* **1989**, *158*, 421.

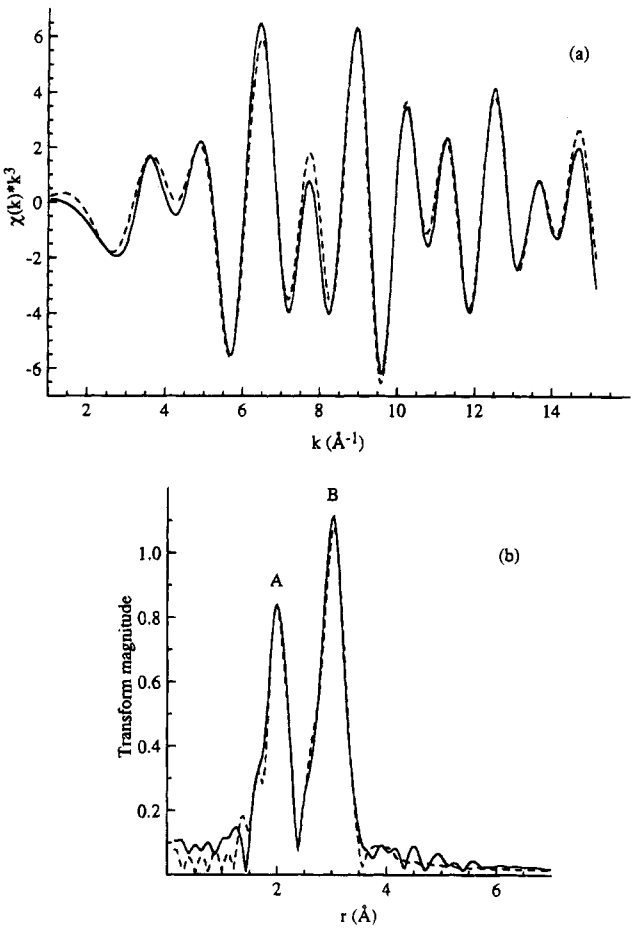

Figure 2. EXAFS spectrum and its Fourier transform of $Tc_2(CO)_{10}$. The solid line is the experimental data, and the dashed line, a best fit.

Table 2. Bond Lengths in $Tc_2(CO)_{10}$ Obtained by X-ray Crystallography[20]

bond	bond length (Å)	bond	bond length (Å)
Tc−C (apical)	1.90	C−O (apical)	1.20
Tc−C (equatorial)	2.00 (av)	C−O (equatorial)	1.12 (av)
Tc−Tc	3.04		

the effect in studies of compounds of the uranyl unit.[25,26] It was therefore anticipated that multiple scattering along the Tc−C−O vector should play an appreciable role in determining the EXAFS of $Tc_2(CO)_{10}$.

Figure 2 shows the EXAFS spectrum and its Fourier transform for $Tc_2(CO)_{10}$. The latter may be interpreted straightforwardly in terms of the X-ray crystal structure. $Tc_2(CO)_{10}$ is isostructural with $Mn_2(CO)_{10}$ and $Re_2(CO)_{10}$ and consists of two $Tc(CO)_5$ moieties linked by a single Tc−Tc bond. The coordination geometry about each Tc is pseudooctahedral, and the $Tc(CO)_5$ units adopt a staggered orientation to give overall D_{4d} symmetry. The bond lengths are given in Table 2, from which it is clear that only two peaks are expected in the Fourier transform of the EXAFS as the Tc−Tc and Tc−O distances are almost the same.

Attempts to fit the experimental EXAFS within a single scattering model using the known interatomic distances proved unsuccessful. While the frequency giving rise to peak A in the Fourier transform was adequately reproduced, it was impossible to obtain a good fit to peak B using one Tc and five O single backscatterers. A theoretical calculation of the EXAFS of $Tc_2(CO)_{10}$ using the FEFF 5 code of Rehr et al.[27,28] was therefore carried out, in order to determine the importance of multiple scattering along the Tc−C−O vector and to obtain phase and amplitude functions for these paths for use in the EXAFS curve fitting.

Table 3. Structural Parameters from EXAFS Curve Fitting of $Tc_2(CO)_{10}$

shell	CN[a]	path degeneracy	r (Å)	Debye−Waller factor (Å²)
Tc−C	5		2.00	0.0030
Tc→C→O[b]		8	3.08[c]	0.0026
Tc→C→O→C[b]		4	3.08[c]	0.0018
Tc−Tc	1		3.13	0.0020

[a] Coordination number. [b] Multiple scattering path. [c] Effective Tc···O distance.

The structural input to FEFF 5 was simplified so as not to distinguish between the slightly different apical and equatorial Tc−C and Tc−O distances. Multiple scattering was found to be extremely important in determining the overall EXAFS, more so than the single scattering Tc···O pathway. If the maximum amplitude predicted for the Tc−C path is arbitrarily set to 100%, then the Tc→C→O (i.e. forward scattering by the C atom) pathway has a maximum amplitude of 94% and the Tc→C→O→C path 63%. The direct Tc···O scattering has an amplitude ratio of only 35%. Hence FEFF 5 provides a clear explanation as to why the experimental EXAFS could not be adequately fitted within the framework of the single scattering model.

Fitting of the experimental EXAFS was therefore attempted using phase and amplitude functions from FEFF 5 for single scattering Tc−C and Tc−Tc pathways and for both single and multiple scattering Tc···O paths. The results are shown in Figure 2 and given in Table 3. The best fit was obtained when the single scattering Tc···O path was omitted entirely and is a significant improvement over the previous approach using only single scattering. Floating the r values caused the fit to converge to a Tc−Tc distance slightly greater than the Tc···O distance and 0.09 Å more than that obtained by X-ray crystallography. Given the number of both single and multiple scattering pathways contributing to peak B, it is unlikely that this discrepancy is significant.

(ii) TcO_2. TcO_2 is believed to be similar to MoO_2 in possessing a distorted rutile structure.[29−32] In MoO_2, the metal atoms are slightly displaced from the centers of the MO_6 units, producing chains with alternating short and long Mo−Mo distances. Powder X-ray diffraction data for TcO_2 have been indexed in terms of a monoclinic MoO_2-type unit cell,[30,31] although there is no general agreement as to the values of the cell parameters.[30] No interatomic distances have been reported for TcO_2.

The electronic structures of transition metal dioxides with rutile and rutile-related crystal structures have received much

(24) O'Day, P. A.; Rehr, J. J.; Zabinsky, S. I.; Brown, G. E. *J. Am. Chem. Soc.* **1994**, *116*, 2938.
(25) Clark, D. L.; Eckberg, S. A.; Newton, T. W.; Palmer, P. D.; Trait, C. D.; Zwick, B. D.; Bucher, J. J.; Edelstein, N. M.; Hudson, E. A.; Kaltsoyannis, N.; Lukens, W. W.; Reich, T.; Shuh, D. K. Manuscript in preparation.
(26) Bucher, J. J.; Edelstein, N. M.; Kaltsoyannis, N.; Lukens, W. W.; Shuh, D. K. Unpublished results.
(27) Mustre de Leon, J.; Rehr, J. J.; Zabinsky, S. I.; Albers, R. C. *Phys. Rev. B* **1991**, *44*, 4146.
(28) Rehr, J. J.; Mustre de Leon, J.; Zabinsky, S. I.; Albers, R. C. *J. Am. Chem. Soc.* **1991**, *113*, 5135.
(29) Greenwood, N. N.; Earnshaw, A. *Chemistry of the Elements*; Pergamon Press: Oxford, U.K., 1984.
(30) Magnéli, A.; Anderson, G. *Acta Chem. Scand.* **1955**, *9*, 1378.
(31) Muller, O.; White, M. B.; Roy, R. *J. Inorg. Nucl. Chem.* **1964**, *26*, 2075.
(32) Rogers, D. B.; Shannon, R. D.; Sleight, A. W.; Gillson, J. L. *Inorg. Chem.* **1969**, *8*, 841.

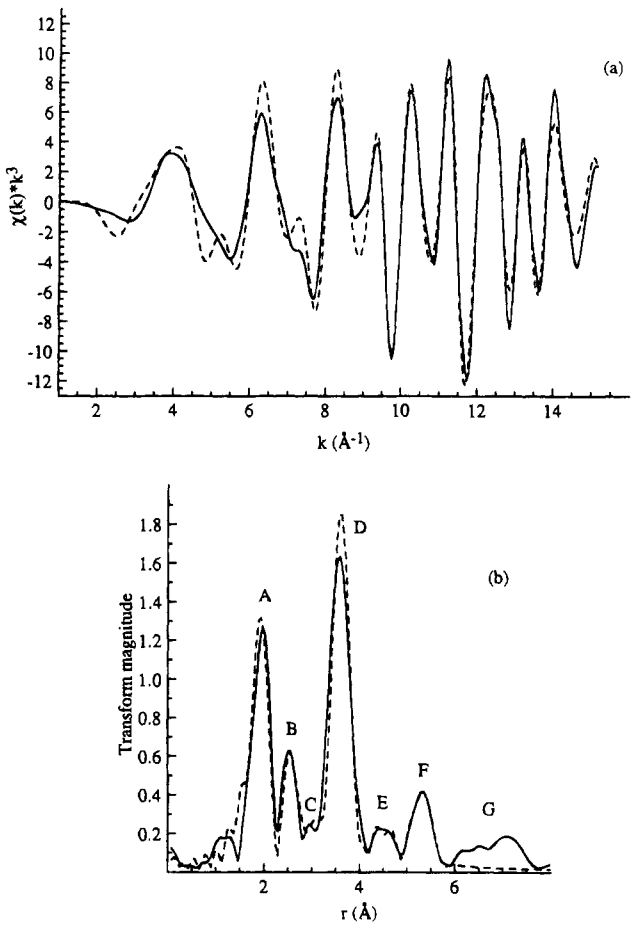

Figure 3. EXAFS spectrum and its Fourier transform of TcO_2. The solid line is the experimental data, and the dashed line, a best fit.

attention,[32-35] in particular the relationship of d electron count and electrical conductivity to structural type. It was therefore decided to investigate the EXAFS of TcO_2 in order to confirm the distorted rutile structure and to establish its relationship to similar MO_2 systems.

Figure 3 shows the EXAFS spectrum and its Fourier transform for TcO_2. It is appreciably more complicated than that of $Tc_2(CO)_{10}$, with six well-resolved peaks (A–F) in the transform between $r = 1.5$ and 6.0 Å. There is also a broad, unresolved peak (G) between 6 and 7.5 Å.

In order to interpret the EXAFS data, the number, type, and location of the backscattering atoms were calculated using the proposed distorted rutile structure[32] as a basis. The results are given in Table 4. There are 88 backscatterers between 1.94 and 6.0 Å and a further 100 between 6.0 and 8.0 Å, and hence caution must be exercised when interpreting Figure 3b. The problem may be simplified considerably by assuming that the contribution of O backscatterers to the EXAFS is negligible beyond the first shell. Support for this assertion is provided by Figure 4, which shows the results of FEFF 5 calculations of the Tc K edge EXAFS for single Tc and O backscatterers at 2.0 and 3.5 Å. The Tc–Tc backscattering dominates the Tc–O except in Figure 4c, which compares the Tc EXAFS from an O atom at 2.0 Å with a Tc at 3.5 Å. For any equal Tc–Tc and Tc–O distances, the O-induced EXAFS is very small in comparison with the Tc contribution.

Table 4. Calculated Tc–Backscatterer Distances in TcO_2[a]

Backscatterer	CN	r (Å)	Backscatterer	CN	r (Å)
O	6	1.94–2.08	Tc	3	4.61–4.85
Tc	1	2.48	Tc	3	4.95–5.15
Tc	1	3.08	Tc	6	5.30–5.39
Tc	4	3.65	Tc	10	5.53–5.69
Tc	4	3.71			

44 Tc between 6 and 8 Å; 50 O between 3.19 and 5.98 Å; 56 O between 6 and 8 Å

[a] Calculations based on unit cell parameters given in ref 32. Space group $P2_1/c$; $a = 5.55$, $b = 4.85$, $c = 5.62$ Å; $\beta = 121.9°$.

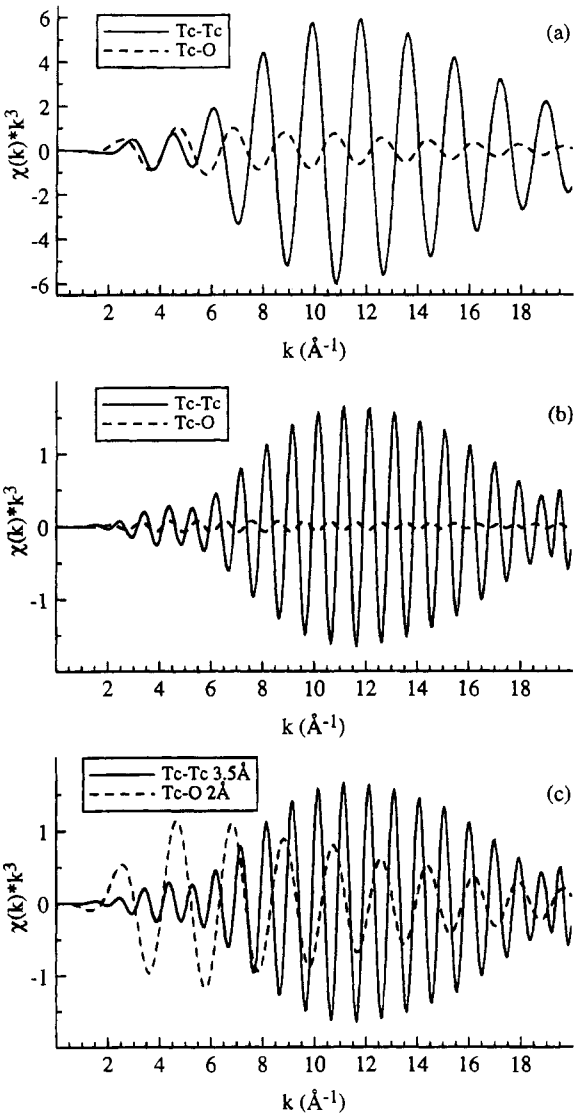

Figure 4. Theoretical Tc K edge EXAFS for single Tc and O backscatterers at (a) 2.0 Å, (b) 3.5 Å, and (c) 2.0 Å (Tc–O) and 3.5 Å (Tc–Tc).

Fitting of the TcO_2 EXAFS was attempted on the basis of the distorted rutile structure, using phase and amplitude functions from FEFF 5. The results are shown in Figure 3 and collected in Table 5. No attempt was made to fit peak G in the Fourier transform as there are too many backscatterers at these r values to produce meaningful results. Although the low-k region (2–9 $Å^{-1}$) is not reproduced perfectly, the data in Table 5 provide strong support for the distorted rutile structure. The closest Tc–Tc distance is *ca.* 0.1 Å longer than expected on the basis of the structure of MoO_2 and the unit cell dimensions of TcO_2.[32] The discrepancy between the r values of Tables 4 and 5 increases slightly at high r, but given the complexity of the

(33) Goodenough, J. B. *Prog. Solid State Chem.* **1971**, *5*, 145.
(34) Beatham, N.; Orchard, A. F. *J. Electron. Spectrosc. Relat. Phenom.* **1979**, *16*, 77.
(35) Cox, P. A. *The Electronic Structure and Chemistry of Solids*; OUP: Oxford, U.K., 1987.

Table 5. Structural Parameters from EXAFS Curve Fitting of TcO_2

shell	CN	r (Å)	Debye–Waller factor (Å^2)	shell	CN	r (Å)	Debye–Waller factor (Å^2)
Tc–O	6	1.98	0.0038	Tc–Tc	3	4.59	0.0065
Tc–Tc	1	2.61	0.0038	Tc–Tc	3	4.77	0.0054
Tc–Tc	1	3.10	0.0035	Tc–Tc	6	5.26	0.0056
Tc–Tc	4	3.64	0.0040	Tc–Tc	10	5.48	0.0084
Tc–Tc	4	3.67	0.0040				

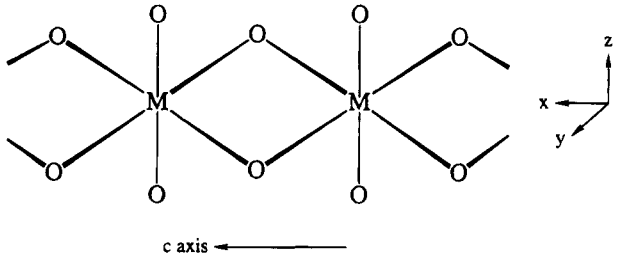

Figure 5. Part of the chain of edge-sharing MO_6 units in the undistorted rutile structure (after Beatham et al.[34]).

experimental spectrum, the reduced accuracy of EXAFS distances at high r, and the uncertainty as to the TcO_2 unit cell dimensions, it is unlikely that these differences are significant.

$Tc_2(CO)_{10}$ is considered to possess a Tc–Tc single bond, with the metal atoms lying 3.04 Å apart.[20] The closest Tc–Tc separation in TcO_2 (2.61 Å) is significantly less than this, suggesting a degree of Tc–Tc multiple bonding. A theoretical framework has been developed by Goodenough and subsequent workers which rationalizes the distortions from the regular rutile structure displayed by a number of transition metal dioxides[32–34] and which accounts for their electrical behavior. The essential features of this model may be understood with reference to Figures 5 and 6. Figure 5 shows part of the chain of edge-sharing MO_6 units in the rutile structure. Even in regular rutile, the MO_6 units are not perfectly octahedral but are distorted in a manner which allows the possibility of M–M bonding along the c axis. In terms of the coordinate system of Figure 5, the metal d_{xy} and d_{z^2} AOs are involved in M–O σ bonding, while the d_{yz} orbital experiences M–O π overlap. The $d_{x^2-y^2}$ orbital may engage in direct M–M σ bonding if the metal atoms are sufficiently close together. The remaining metal d AO, the d_{xz}, is predominantly M–O π bonding but M–M π interaction is also possible.

Qualitative orbital diagrams depicting varying degrees of M–M interaction are shown in Figure 6. TiO_2, which of course possesses the regular rutile structure, is formally a d^0 compound with sufficient electrons to fill completely the M–O σ and π-bonding orbitals as shown in Figure 6a. The lowest unoccupied levels consist of a band formed by the essentially nonbonding $d_{x^2-y^2}$ metal AOs (labeled M–M σ) together with the M–O π^* orbitals. The latter are composed predominantly of the metal d_{yz} and d_{xz} AOs. Replacing Ti with V or Nb provides an additional electron per metal atom which, on the basis of Figure 6a, would partially fill the M–M σ/M–O π^* band system. This is indeed the case in VO_2 above 340 K and NbO_2 above 1070 K, where both compounds have the regular rutile structure and exhibit metallic conductivity. Below these temperatures, both oxides become semiconducting and distort so as to produce the alternating short and long M–M distances described above for MoO_2. A qualitative rationalization of this is given in Figure 6b, in which a M–M σ band separates from the M–M σ^*/M–O π^* levels. This corresponds to the trapping of two metal-based electrons between pairs of metal atoms, i.e. the creation of localized M–M σ bonds.

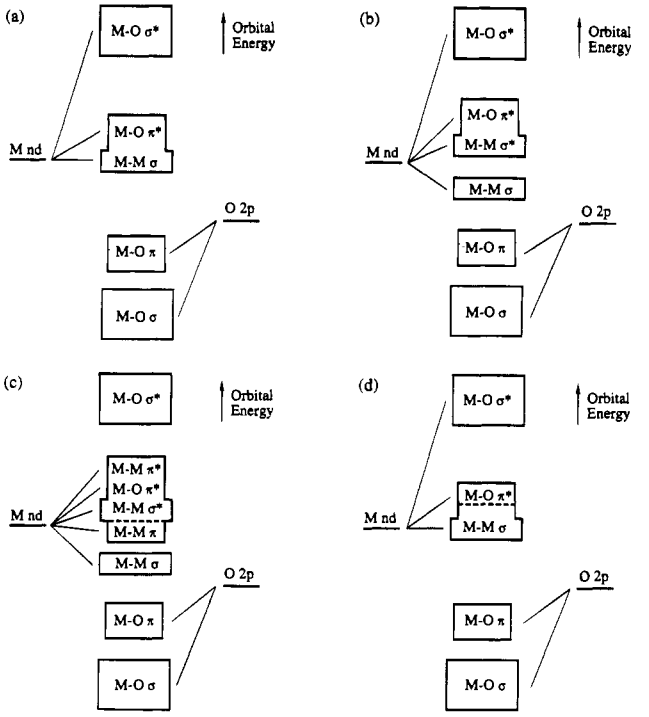

Figure 6. Qualitative orbital diagrams for transition metal dioxides with rutile-related structures.

MoO_2 possesses one more d electron per metal atom than NbO_2 and exhibits metallic conductivity. At first glance, this would appear to be consistent with Figure 6b in that the extra electrons occupy the M–M σ^*/M–O π^* band, which is then partially filled. Unfortunately the closest M–M separation in NbO_2 is 2.80 Å but only 2.51 Å in MoO_2,[32] suggesting that the additional electrons in the group VIA compound play at least some role in M–M bonding. A mechanism for this is provided by the metal d_{xz} AOs which are principally M–O π bonding but which may also experience M–M π interaction if the metal atoms are close enough together. MoO_2 may therefore be rationalized by invoking a greater M–M π bonding role for the d_{xz} orbitals. Figure 6c represents this situation but essentially corresponds to a relabeling of the M–O π^* band.

The d^4 RuO_2 also exhibits metallic conductivity but, unlike NbO_2 and MoO_2, possesses the regular rutile structure with Ru–Ru distances of 3.11 Å. It may be explained in terms of Figure 6d, in which the M–M σ and M–M σ^* levels of Figure 6b,c have become filled, resulting in little net M–M interaction. The M–M σ/M–O π^* band is only partially occupied, accounting for the metallic conductivity.

Our EXAFS results clearly indicate that TcO_2 has a distorted rutile structure similar to that of MoO_2. The short Tc–Tc distance of 2.61 Å suggests that the bonding in TcO_2 is best represented by Figure 6c, with the Tc $4d_{xz}$ AOs engaging in both M–O and M–M π bonding. In this respect, TcO_2 is similar to α-ReO_2, which also possesses a monoclinic distorted rutile structure.[32,36,37] The short Re–Re distance is not known accurately but is approximately 2.49 Å. ReO_2 exhibits metallic conductivity, as expected on the basis of Figure 6c. By comparison with MoO_2 and ReO_2, TcO_2 is also expected to have metallic conductivity, but there are no reports of its electrical properties.

(36) Magnéli, A.; Andersson, G.; Blomberg, B.; Kihlborg, L. *Anal. Chem.* **1952**, *24*, 1998.

(37) A high-temperature, orthorhombic modification of ReO_2 is also known. It is possible that a similar situation exists for TcO_2, which could explain the discrepancies in the reported unit cell parameters.

The 2.61 Å Tc−Tc separation may be rationalized in terms of the balance between M−M σ and M−M π bonding. On moving from the d^2 MoO_2 to the d^3 TcO_2, the M−M π/M−M σ^*/M−O π^* band contains additional electrons, which may weaken the Tc−Tc σ bonding by partially populating the M−M σ^* levels. This results in a lengthening of the M−M bond, a trend which is completed in RuO_2 when the M−M σ^* levels are filled and no net M−M bonding occurs.

Concluding Remarks

While it is recognized that the effective charge on an atom is only one of several factors contributing to the position of its X-ray absorption edge, our results demonstrate a strong correlation between formal oxidation state and Tc K edge energy in a diverse series of Tc compounds. It would therefore seem prudent to view X-ray absorption edge energies as valuable pieces of information for determining the electronic environment of absorbing atoms, although conclusions should never be based solely upon edge shift data.

The valuable contribution that theoretical methods can make to the interpretation of EXAFS has been demonstrated by our study of $Tc_2(CO)_{10}$. Although the need to account for multiple scattering pathways was recognized in a qualitative sense, a satisfactory understanding of the experimental data was possible only with theoretically determined phase and amplitude functions for the multiple scattering paths. Theoretically generated EXAFS were also of use in justifying our approach to the interpretation of the complex experimental data acquired for TcO_2, which has been shown to resemble other transition metal dioxides in possessing a variant of the rutile structure. We believe that the judicious application of theoretical techniques has an important role to play in enhancing our understanding of the X-ray absorption process.

Acknowledgment. This work was supported in part by the Director, Office of Energy Research, Office of Basic Energy Sciences, Chemical Sciences Division of the U.S. Department of Energy under Contract No. DE-AC03-76SF00098. The work was performed at the SSRL which is operated by the U.S. Department of Energy, Office of Basic Energy Sciences, Divisions of Chemical Sciences and Materials Science. The SSRL Biotechnology Program is supported by the NIH, Biomedical Resource Technology Program, Division of Research Resources. N.K. thanks the EPSRC/NATO for a postdoctoral fellowship.

IC940847U